Nuclear Materials and Energy 12 (2017) 882–886

Contents lists available at ScienceDirect

Nuclear Materials and Energy

journal homepage: www.elsevier.com/locate/nme

High power neon seeded JET discharges: Experiments and simulations

G. Telesca[a,*], I. Ivanova-Stanik[b], R. Zagórski[b], S. Brezinsek[c], A. Czarnecka[b], P. Drewelow[d], C. Giroud[e], A. Huber[c], S. Wiesen[c], M. Wischmeier[f], JET contributors[1]

[a] Department of Applied Physics, Ghent University, B-9000 Gent, Belgium
[b] Institute of Plasma Physics and Laser Microfusion, Warsaw, Poland
[c] Institut fuer Energie-und Klimaforschung-Plasmaphysik Foschungszentrum Juelich GmbH, Juelich, Germany
[d] Max-Planck Institut fuer Plasmaphysik, D-17491 Greifswald, Germany
[e] CCFE Culham, Abingdon, Oxon, OX14 3DB, UK
[f] Max-Planck Institut fuer Plasmaphysik D-85748, Garching bei Muenchen, Germany

ARTICLE INFO

Article history:
Received 12 July 2016
Revised 29 September 2016
Accepted 12 October 2016
Available online 26 October 2016

Keywords:
Tokamak
Integrated modeling
Core plasma
Edge plasma

ABSTRACT

A series of neon seeded JET ELMy H-mode pulses is considered from the modeling as well as from the experimental point of view. For two different Ne seeding rates and two different D puffing gas levels the heating power, P_{heat}, is in the range 22–29.5 MW. The main focus is on the numerical reconstruction of the total radiated power (which mostly depends on the W concentration) and its distribution between core and divertor and of Z_{eff} (which mostly depends on the Ne concentration). To model self-consistently the core and the SOL two input parameters had to be adjusted case by case: the SOL diffusivity, D_{SOL}, and the core impurity inward pinch, v_{pinch}. D_{SOL} had to be increased with increasing Γ_{Ne} and the level of v_{pinch} had to be changed, for any given Γ_{Ne}, according to the level of P_{heat}: it decreases with increasing P_{heat}. Since the ELM frequency, f_{ELM}, is experimentally correlated with P_{heat}, (it increases with P_{heat}) the impurity inward pinch can be seen as to depend on f_{ELM}. Therefore, to maintain a low v_{pinch} level (i.e. high f_{ELM}) Γ_{Ne}/P_{heat} should not exceed a certain threshold, which slightly increases with the Γ_D puffing rate. This might lead to a limitation in the viability of reducing the target heat load by Ne seeding at moderate Γ_D, while keeping Z_{eff} at acceptably low level.

1. Introduction

For a fully metallic device like JET with the ITER-Like-Wall (W divertor, Be wall) impurity seeding is an essential technique to reduce the power load to the targets, via enhanced edge radiation. Indeed, the naturally occurring radiation losses are low (~25–30% of the heating power), as compared to those with carbon target (~50%). Significant progress has been made at JET in reducing the heat and particle load to the divertor plates by injecting light impurities as N, Ne and Ar, expecially in the ITER-relevant vertical-target configuration (low and high delta), at $I_p = 2.5$ MA and $B_t = 2.7$ T [1,2].

In contrast to Ne injection with carbon PFC, Ne seeding in ILW causes significant changes in the radiation pattern also in the core plasma. Generally, Ne injection not only leads to enahanced radiation in the SOL and around the X-point, as for carbon sorroundings, but also to increased tungsten release, with related enhanced core radiation and possible reduced ELM frequency. This can cause excessive impurity residence time and may lead to impurity accumulation [3]. This paper, based on experimental JET data as well as on core-SOL self-consistent modelling, is focusing on the relation between the level of Ne seeding rate and the change in the impurity transport.

Among a number of experiments carried out recently, a series of Ne seeded low-delta ELMy H-mode pulses with heating power, P_{heat}, up to 29.5 MW and with two different levels of seeding rate as well of gas fueling is considered in the present study.

We have focused our interest on the global radiation properties of these pulses as well as on impurity transport and on the effective charge Z_{eff}, neglecting other aspects of these discharges, as, for example, the confinement properties (see ref [1,2,4]). In particular, an anomalously high Z_{eff} is observed to occour when, for a given level of P_{heat}, Ne seeding exceeds a certain threshold. In this case, indeed, the incremental Z_{eff} caused by Ne seeding is higher than that expected from the related incremental radiated power. It is

* Corresponding author.
E-mail address: g.telesca@fz-juelich.de (G. Telesca).

[1] *see the Appendix of F. Romanelli* et al., *Proceedings of the 25th IAEA Fusion Energy Conference 2014, Saint Petersburg, Russia*.

http://dx.doi.org/10.1016/j.nme.2016.10.012

also observed that the ELM activity decreases significantly, while the plasma enegy remains unchanged.

In these pulses the volume average density, $\langle n_e \rangle$, is in the range $6–7 \times 10^{19}/m^3$, P_{heat} from 22 to 29.5 MW (NBI+ICRH), the two steps in Ne seeding rate are 5 and 12×10^{21} e/s and the two steps in D_2 gas fuelling rate are 1.9 and 3.7×10^{22}/s. The radiated power fraction ($f_{RAD} = P_{rad}{}^{TOT} / P_{heat}$) changes from 0.47 to 0.61 and the ratio of radiated power in the SOL to the total one ($P_{rad}{}^{SOL} / P_{rad}{}^{TOT}$) is between 0.35 and 0.43. The main aim of this work consists in reproducing numerically, for each pulse, the electron temperature, $T_e(r)$ and density $n_e(r)$ profiles in the core plasma, $P_{rad}{}^{TOT}$, $P_{rad}{}^{SOL}/P_{rad}{}^{TOT}$ and Z_{eff} by changing a limited number of inputs: $\langle n_e \rangle$, P_{heat} and Γ_{Ne} (see next section). It is worth mentioning that for each "shot-point" the simulation outputs shown in Section 3 are obtained from a single run, i.e. all the quantities are calculated simultaneously. Indeed, numerical simulation of these discharges is being made in view of finding the best conditions leading to high f_{rad} together with acceptable Z_{eff} for a situation as close as possible to a real experimental pulse,

For the simulations we have used COREDIV code [5], which self-consistently couples the plasma core (1-D) with the plasma edge (2-D) and the main plasma with impurities. Indeed, both the impurity ionization and radiation losses contribute to the establishment of the electon density and temperature profiles. Although the simulations refer to the inter-ELM phase of the discharges, since production as well as flushing out of W due to ELMs is not accounted for in the present model, the numerical results might be compared with experimental data averaged over several ELM periods [6,7].

Section 2 deals with the description of the numerical model COREDIV. In Section 3 the numerical results are compared with experimental data. Discussion and summary are made in Section 4.

2. The COREDIV code

Since the energy balance depends strongly on the coupling between the bulk and the scrape-off layer (SOL) plasma, modeling requires the transport problem to be addressed in both regions simultaneously. The physics model used in the COREDIV code is based on a self-consistent coupling of the radial transport in the core to the 2D multifluid description of the SOL.

In the core, given as code input the volume average electron density $\langle n_e \rangle$, the 1D radial transport equations for bulk ions, for each ionization stage of each impurity ions (Be, Ne and W) and for the electron and ion temperature are solved. The electron and ion energy fluxes are defined by the local transport model proposed in ref. [8] which reproduces a prescribed energy confinement law. In particular, the anomalous heat conductivity is given by the expression $\chi_{e,i} = C_{e,i}{}^* \, a^2/\tau_E{}^* \, F(r)$ where r is the radial coordinate, a is the plasma radius, τ_E is the energy confinement time defined by the ELMy H-mode scaling law and the coefficient ($C_e = C_i$) is adjusted to have agreement between calculated and experimental confinement times. The parabolic-like profile function $F(r)$, which may slightly change from run to run in order to match with the actual profiles of the experimental pulse to be modelled, can be modified at the plasma edge to provide for a transport barrier of chosen level. The main plasma ion density is given by the solution of the radial diffusion equation with diffusion coefficients $D_i = D_e = 0.2\chi_e$, as in ref. [8]. Note, however, that the solution of the diffusion equation is largely independent of the exact value of D_e/χ_e. Indeed, a change in D_e/χ_e causes a consistent change in the source term, since the average electron density is a COREDIV input. An anomalous pinch velocity can be applied to the main ions to account for possible density peaking. In all these simulations $v_{pinch}(main) = -0.05$ m/s. For the auxiliary heating, parabolic-like deposition profile is assumed $P_{aux}(r) = P_0 \, (1-r^2/a^2)^y$ where y is in the range 1.5–3, depending on the quality of the auxiliary heating, NBI or/and ICRF. For all the pulses considered in this study $y = 2$, since the fraction of ICRH power level to the total power is nearly constant, $P_{ICRH}/P_{NBI} = 0.2$. The impurity diffusion coefficient is set to be equal to that of the main ions and an anomalous impurity pinch is given as input, in the range 0 to -1 m/s for the pulses here considered (see Section 3). The pinch profile increases linearly, in absolute value, from zero at the plasma centre to its maximum (the value we quote) at $r = a$.

In the SOL the 2D boundary layer code EPIT [9] is used, which is primarily based on Braginskii-like equations for the background plasma and on rate equations for each ionization stage of each impurity species (Be, Ne and W in these simulations). An analytical description of the neutrals is used, based on a simple diffusive model. COREDIV takes into account the plasma (D, Be and seeded impurities) recycling in the divertor as well as the sputtering processes at the target plates including W sputtering by deuterons, self-sputtering and sputtering due to seeded impurities. (For deuterium and neon sputtering and tungsten self-sputtering the yields given in Refs. [10,11] are used). W self-sputtering accounts for about 10% of the total W release, for the simulations presented in this paper. The recycling coefficient is an external parameter which in COREDIV depends on the level of the electron density at the separatrix, n_{e_sep}, given as an input, and increases with increasing n_{e_sep}.

A simple slab geometry (poloidal and radial directions) with classical parallel transport and anomalous radial transport ($D_{SOL} = \chi_i = 0.5 \, \chi_e$, where χ_e ranges typically 0.5–1.5 m^2/s), is used and the impurity fluxes and radiation losses by impurity ions are calculated fully self-consistently. Although the values of the transport coefficients in the SOL are generally quite comparable to those at the separatrix, in the present simulations the value of D_{SOL} is set arbitrarily (in the range 0.4–0.7 m^2/s) in order to match with the core-SOL distribution of the radiated power, depending on the different levels of Ne seeding rate (see next section). All the equations are solved only from the midplane to the divertor plate, assuming inner-outer symmetry of the problem. This implies that the experimental in–out asymmetries, observed especially at high density-high radiation level, are not reproduced in COREDIV results. However, for all the different situations examined so far (with carbon plates and with the ILW, and with different seeding levels [6,12]) the COREDIV numerical reconstructed total radiation in the SOL matches well with the total experimentally measured SOL radiation, indicating that for JET conditions the edge-core COREDIV model can describe the global trend of this important quantity.

The coupling between the core and the SOL is made by imposing continuity of energy and particle fluxes as well as of particle densities and temperatures at the separatrix. The computed fluxes from the core are used as boundary condition for the SOL plasma. In turn, the values of temperatures and of densities calculated in the SOL are used as boundary conditions for the core module

3. Experiments and simulations

Fig. 1 shows some time-dependent traces of the four pulses. In JPN 87,190 (first from left) P_{heat} (NBI +RF) is 22MW, $\Gamma_{Ne} = 0.5$ 10^{22}e/s and for $t < 14.5$ s with $\Gamma_D = 4.0 \times 10^{22}$ e/s ELM activity is stationary with $f_{ELM} = 40$ Hz, $Z_{eff} = 1.9$ and $f_{RAD} = 0.47$. Starting from $t = 14.5$ s the gas fueling decreses to $\Gamma_D = 1.9 \times 10^{22}$ e/s and the ELM behavior is non-stationary, alternating periods of ELM activity with $f_{ELM} = 40$ Hz with ELMy-free periods. Correlated also with a slight decrease in $\langle n_e \rangle$, Z_{eff} goes up to 2.4 and $f_{RAD} = 0.52$. In JPN 87,191 (second from left) the two gas fuelling steps are interchanged in time, but their values are quite similar to those in the previous pulse, while remains $\Gamma_{Ne} = 0.5$ 10^{22}e/s. With P_{heat}

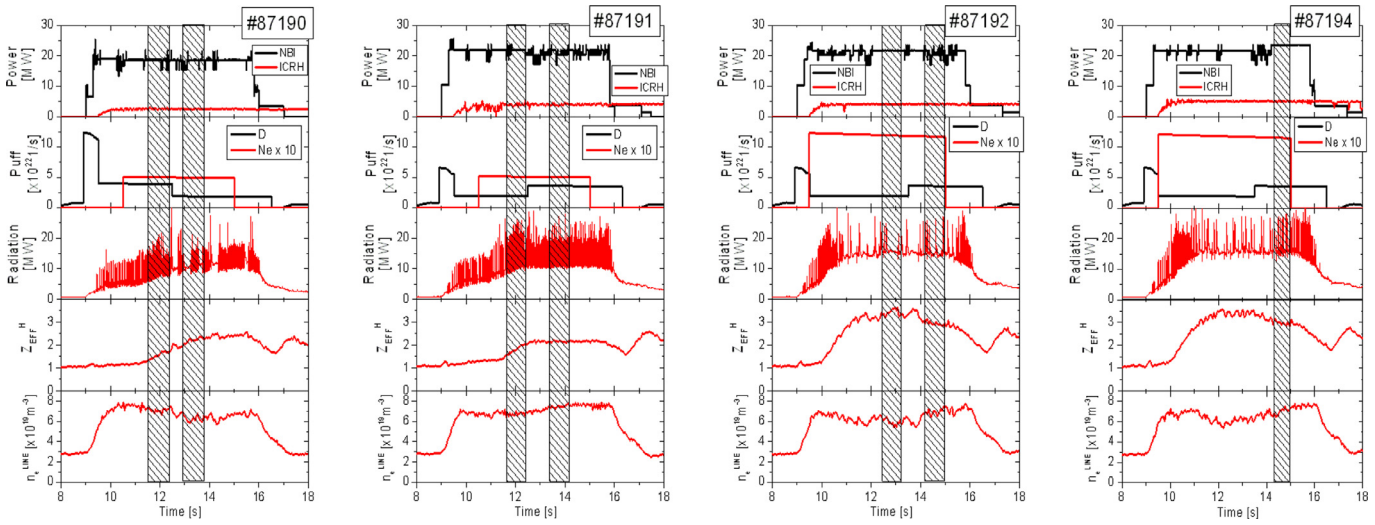

Fig. 1. Experimental time traces of the four pulses examined. The seven time slices of the simulated "shot points" are shown.

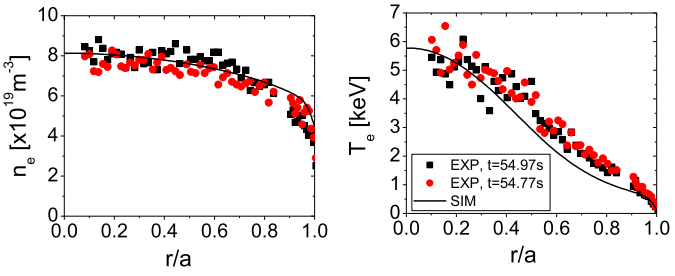

Fig. 2. Experimental (HRTS) and reconstructed T_e and n_e profiles for JPN 87,194 t = 14.9 s.

= 26 MW, ELM activity is stable at both Γ_D, f_{ELM} = 60–70 Hz, with Z_{eff} around 2 and f_{RAD} = 0.54 and 0.47, respectively. In JPN 87,192 (third), Γ_{Ne} = 1.2 10^{22}e/s while all the other inputs are keept as in the previous pulse. ELM activity is non-stable with f_{ELM} = 5–9 Hz, Z_{eff} in the range 3.4–3.0 and f_{RAD} around 0.55. Adding 1 MW of ICRH, as in JPN 87,194 (fourth) up to t = 14.5 s, does not improve the situation with respect to Z_{eff} and f_{ELM}. At t = 14.5 s, 2 more megawatts NBI are added resulting in P_{heat} = 29.5 MW. Even though no significant improvement is observed with respect to Z_{eff}, a tendency towards a more regular ELM behavior might be seen, with f_{ELM} which becomes 15 Hz.

Before comparing and discussing the global quantilties of the core and the SOL, the experimental (from High Resolution Thomson Scattering diagnostic) and simulated T_e and n_e profiles in the core plasma of one of the four pulses here considered (JPN 87,194 t= 14.9 s) are shown in Fig. 2, as an example. Although some discrepancies experiment-simulation can be seen, these discrepancies are marginally influent for the numerical reconstruction of the global quantities of the core plasma. Indeed, due to the rather flatness of the n_e profile, small differences experiment-simulation in the T_e profile in the confined plasma cause a marginal effect on the level of the reconstructed radiated power. On the other hand, recalling that impurity transport is set to be anomalous in the present version of COREDIV (see Section 2), the differences experiment-simulation in the T_e profile gradients are also of minor concern.

Since from tomographic reconstruction it is difficult to distinguish, within the uncertainties in space of the measurement, the radiation emitted in the core from that in the SOL, especially in the vicinity of the X-point, we have followed a procedure, used at JET [13], by which all the power radiated below Z= −1 m is considered as divertor radiation. Since neon radiates partly in the SOL and partly at the very edge of the plasma core around the X-point, this assumption turns out to include the total radiation emitted by Ne in what we call "experimental divertor radiation". Being the core module of COREDIV one-dimensional (see above), the simulated Ne radiation inside the separatrix is poloidally uniformly distributed and it is located, as in the experiment, at the very edge of the core. To compare consistently simulations with measurements we have therefore added the COREDIV neon radiation emitted at the very edge of the core to the COREDIV SOL radiation, resulting in the "simulated divertor radiation" . In Fig. 3 the seven "shot-points" have been ordered according to P_{heat} and the four points referring to P_{heat} = 26 MW have been slithly displaced in P_{heat} to avoid superposition. The points referring to Γ_{Ne} = 1.2 10^{22}e/s have been drawn with larger symbols. Fig. 3a,b,c show that P_{rad}^{TOT}, P_{rad}^{SOL} / P_{rad}^{TOT} and Z_{eff}, which are the basis of our comparison experiment-simulation, have been numerically reconstructed with good accuracy. Fig. 3d shows that the experimental f_{RAD} (as well as the simulated one) does not increase significantly by increasing Γ_{Ne}, which, however, leads to a clear increase in Z_{eff}. This point is made more clear by noting that the quantity P_{rad}^{TOT} / (Z_{eff} −1) x n_e^2 [14] drops nearly by a factor of 2 at high Γ_{Ne} (Fig. 3e). Figs. 3f and g show that the experimental volume averaged W concentration (from SXR) and the central plasma Ne^{10+} ion concentration (from CXRS) match with the simulated ones, considering the error bar (order 20%) of the measurements. The electron temperature at the outer stike point, measured by LP (with significant error bar), is in the range 6–9 eV (9 eV for the pulse at 26 MW with $\Gamma_{Ne} = 0.5 \times 10^{22}$ e/s), while the simulated one is in the range 4–6.5 eV Considering that the experimental T_e at the inner strike point is about 2–3 eV lower than at the outer one, the discrepancy experiment-simulation is consistent with the COREDIV SOL model, in which in-out symmetry is assumed (only one target plate, see Section 2). Fig. 3h shows that high Γ_{Ne} level is an effective tool to reduce the power to the plate also at high P_{heat}. The simulated recycling D fluxes, Γ_D, are about a factor of 2 higher than the LP experimental ones. This depends on the value of the COREDIV input electron density at the separatrix, n_{e_sep}. Indeed, the recycling deuterium flux is not a free parameter in the model (see Section 2), but it is linked to the input value of n_{e_sep}, which, in all these simulations is in the range 0.45 – 0.5 x $\langle n_e \rangle$. [6].

Together with P_{heat}, $\langle n_e \rangle$ and Γ_{Ne} two other input parameters have been changed "shot-point" to "shot-point" in order to

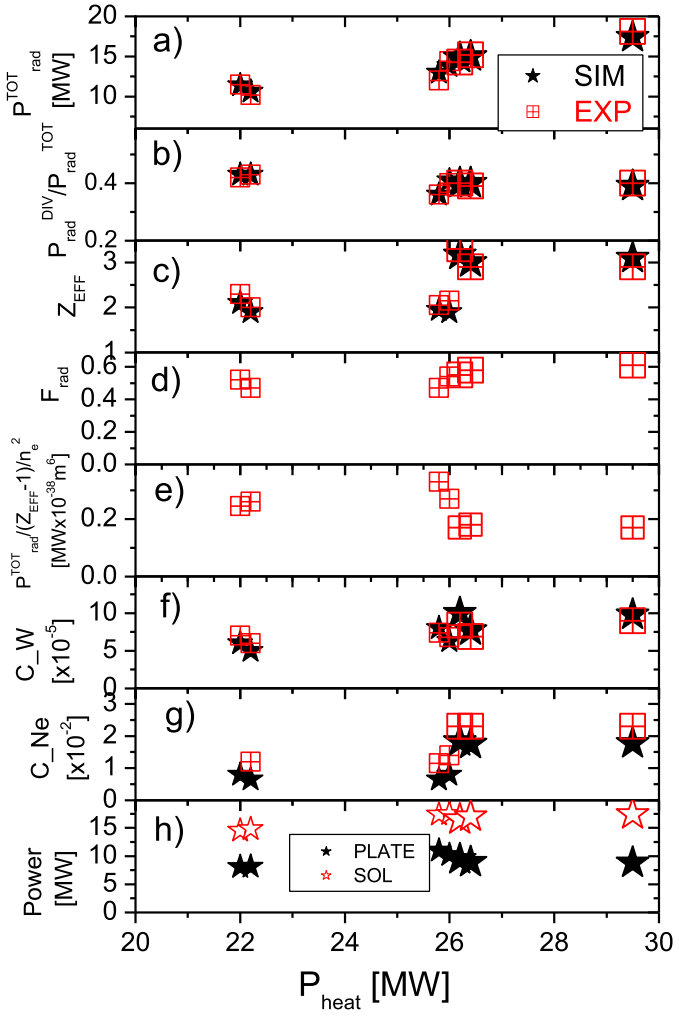

Fig. 3. Comparison experiment-simulation for the seven "shot points" here considered. See text.

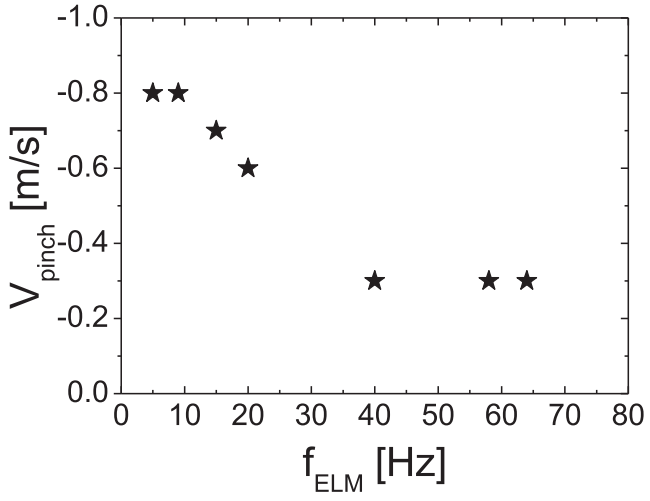

Fig. 4. Numerical pinch velocity vs. experimental ELM frequency.

match simulations with experiments: the perpendicular SOL diffusivity D_{SOL} and the anomalous impurity pinch v_{pinch}. Differently from modelling of unseeded pulses with $D_{SOL} = 0.25$ m^2/s, it has been set $D_{SOL} = 0.45$ m^2/s for the points at $\Gamma_{Ne} = 0.5 \times 10^{22}$e/s and D_{SOL} up to 0.70 m^2/s for the points at $\Gamma_{Ne} = 1.2 \times 10^{22}$e/s. This dependence of D_{SOL} on the level of Γ_{Ne} is made to match the simulated with the experimental P_{rad}^{SOL}. To match both the simulated P_{rad}^{core} (i.e. P_{rad}^{TOT} - P_{rad}^{SOL}) and Z_{eff} with the experimental data, v_{pinch} had to be changed from −0.3 to −0.8 m/s. It might be observed (see Fig. 3f) that, in contrast to c_{Ne}, c_W is relatively insensitive to the application of a high v_{pinch} for the pulses at higher Γ_{Ne}. This depends basically on the fact that, being W highly collisional in the SOL (more than neon), a further decrease in the SOL temperature leads to a change in the balance between frictional and thermal forces in the divertor, resulting in a screening effect more pronounced for W than for Ne. In other words: increasing Γ_{Ne}, the W flux to the separatrix is reduced more than that of Ne while W and Ne suffer the same inward pinch in the confined plasma.

It turns out that v_{pinch} is correlated with f_{ELM}, as seen in Fig. 4. It has to be pointed out, however, that there is no experimental evidence of change in impurity density peaking with decreasing f_{ELM} and that v_{pinch} is simply a numerical tool introduced to change the impurity dwell time. In fact, the same results reported in Fig. 3 can be numerically reproduced by keeping the impurity inward pinch constant ($v_{pinch} = -0.3$ m/s) and by reducing the ratio of the impurity diffusion coefficient in the core plasma to that of the main ions, $D_{imp\text{-}core}/D_{\text{main ions}}$, from 1to 0.4.

With respect to the mechanism responsible for the reduced f_{ELM} at higher Ne seeding rate it seems reasonable to relate the drop of f_{ELM} with the little increase of the radiated power in the main plasma volume. With larger core radiation, more time is needed to restore the pedestal with the heat flow from the plasma core after an ELM crash [15].

It is worth pointing out that it was not possible to model satisfactorily the three ¨ shot points¨ at higher Γ_{Ne} by increasing in COREDIV the Γ_{Ne} by a factor of 2.4 with respect to that of the four ¨shot points¨ at lower Γ_{Ne}, as in the experimental Ne inlet valve signals (see Fig. 1). Match of P_{rad} and of its distribution between core and SOL, of Z_{eff} and of the impurity concentrations was only possible by increasing Γ_{Ne} by a factor of 1.75–1.85. The reasons for this discrepancy are not fully clear, so far. Among many possibilities, this might be linked to the over-simplified COREDIV geometry of the SOL, which does not account for the divetor closure of the vertical target configuration of these pulses, with possible related changes in divertor compression, hence also in pumping efficiency, with increasing Γ_{Ne}.

4. Discussion and summary

Using the actual steady-state version of COREDIV it is not possible to simulate the effect on W release caused by single ELMs. However, for T_{e_pl} above 3–4 eV the W sputtering yield by Ne together with that by Be and by W self-sputtering provide a simulated W flux, which is comparable to that experimentally observed for the most common JET ELMy H-mode situations, once the data are averaged over times $\tau_A >> 1/f_{ELM}$ [6]. Indeed, in JET ELMy-H mode the experimental Γ_W is found to be in the range 3–9 × 10^{19}/s [16,17], as in COREDIV simulations. In particular, for this series of pulses the intensity of the WI emission line at 401 nm, measured at the outer divertor, shows a slight increase (up to about 30%) with increasing P_{heat}, but it remains nearly stationary with increasing Γ_{Ne}, at constant P_{heat}, in agreement with the calculated COREDIV total W fluxes, which increase from about 7 to 9.5 × 10^{19}/s. Indeed, adding more neon at low T_{e_pl} leads to a reduced W sputtering yield while increasing P_{heat} leads to an enhanced W yield.

The necessity of introducing in the simulations an anomalous inward pinch to match experiment-simulation for the pulses at low

f_{ELM} is correlated with the impurity flushing out mechanisms by ELMs [15], and, specifically, with the experimentally observed decrease in W density in the core plasma for f_{ELM} above 40 Hz [17].

In spite of the inner-outer symmetry assumption and of the analytical description of the neutrals which both might hamper the validity of the SOL model especially for situations close to detachment, the global properties of the SOL, as the radiated power and by consequence the average electron temperature at the plate, are sufficiently well numerically reproduced, due also to the adjustement of the particle diffusion coefficient in the SOL, D_{SOL}. The change in D_{SOL} is a technical tool to fitting the numerical P_{rad}^{SOL} with the experimental one and it reflects the increase in collisionality with decreasing the divertor temperature [1].

Experiments and COREDIV modelling indicate that Ne seeding is an efficient method to maintain the power load to the target plates at an acceptable level also at high P_{heat} (order 30 MW) in JET-ILW pulses. However, the level of Γ_{Ne} should be modulated according to the level of Γ_D and of P_{heat} to maintain Z_{eff} at acceptable values. Indeed, when for given Γ_D and P_{heat} the neon seeding rate exceeds a certain treshold, COREDIV simulations indicate that an inward impurity pinch is triggered, esperimentally related to the reduction in the ELM activity.

The simplifying assumptions made in the SOL and in the core of COREDIV in order to model self-consistently the complex interaction core-edge plasma certainly attenuate the validity of the quantitative numerical results. However, the modeling of the pulses here considered indicates a clear trend and suggests, for given P_{heat} and Γ_D, a limit in the level of Γ_{Ne}.

Acknowledgements

One of the authors (G.T.) wishes to thank both referees for their constructive comments.

This work has been carried out within the framework of the EUROfusion Consortium and has received funding from the Euratom research and training programme 2014-2018 under grant agreement No 633053. The views and opinions expressed herein do not necessarily reflect those of the European Commission.

This scientific work was financed within the Polish framework of the scientific financial resources allocated for realization of the international co-financed project.

References

[1] M. Wischmeier, J. Nucl. Mater. 463 (2015) 22 and 25th IAEA Conference 2014, P. EX/7-2, St. Petersburg, Russia.
[2] C. Giroud, Nucl. Fusion 53 (2013) 113025 and 25th IAEA Conference 2014. EX/P5-25, St. Petersburg, Russia.
[3] T. Puetterich, Plasma Phys. Control. Fusion 55 (2013) 124036.
[4] A. Huber, J. Nucl. Mater. 463 (2015) 445.
[5] R. Zagorski, et al., Nucl. Fusion 53 (2013) 073030.
[6] G. Telesca, et al., Contrib. Plasma Phys. 54 (4–6) (2014) 347–352, doi:10.1002/ctpp.201410052.
[7] G. Telesca, et al., J. Nucl. Mater. 463 (2015) 577–581, doi:10.1016/j.jnucmat.2014.11.024.
[8] J. Mandrekas, W.M. Stacey, Nucl. Fusion 35 (1995) 843.
[9] R. Zagorski, J. Tech. Phys. 37 (1996) 7.
[10] Y. Yamamura et al., Report of the IPP Nagoya, IPPJ-AM-26 (1083).
[11] C. Garcia-Rosales, et al., J. Nucl. Mater. 218 (1994) 8–17.
[12] G. Telesca, et al., Plasma Phys. Control. Fusion 53 (2011) 115002.
[13] A. Huber, et al., in: 41st EPS Conference on Plasma Physics, 2014, p. 1.031.
[14] G. Telesca, et al., Nucl. Fusion 40 (2000) 1845.
[15] R. Dux, et al., J. Nucl. Mater. 390-391 (2009) 85.
[16] S. Brezinsek, et al., in: 57th APS Plasma Physics, Savannah, Vol. 60, 2015, p. T06.0007.
[17] N. den Harder, et al., Nucl. Fusion 56 (2016) 026014.